

# Programming the Shape Transformation of a Composite Hydrogel Sheet via Erasable and Rewritable Nanoparticle Patterns

Hongyu Guo,<sup>†</sup> Jian Cheng,<sup>‡</sup> Kuikun Yang,<sup>†</sup> Kerry Demella,<sup>§</sup> Teng Li,<sup>‡</sup> Srinivasa R. Raghavan,<sup>§</sup> and Zhihong Nie<sup>\*,†,||</sup>

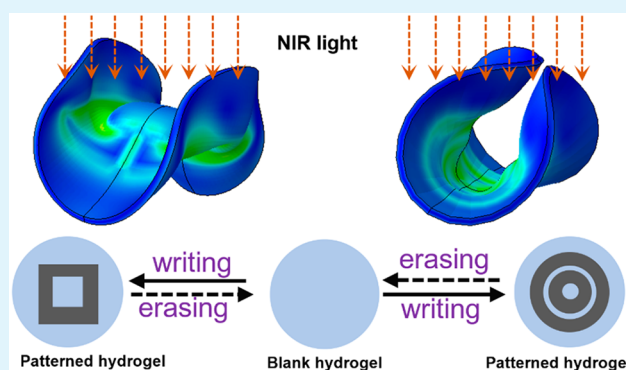
<sup>†</sup>Department of Chemistry and Biochemistry, <sup>‡</sup>Department of Mechanical Engineering, and <sup>§</sup>Department of Chemical and Biomolecular Engineering, University of Maryland, College Park, Maryland 20742, United States

<sup>||</sup>State Key Laboratory of Molecular Engineering of Polymers, Department of Macromolecular Science, Fudan University, Shanghai 200438, P.R. China

## Supporting Information

**ABSTRACT:** Hydrogels with shapes that can be adapted to their environment have attracted great attention from both academia and industry. We report herein a new and robust strategy to reprogram the light-induced shape transformation of a thermoresponsive composite hydrogel sheet with erasable and rewritable patterns of iron oxide nanoparticles as photothermal agents. Numerous distinct and reversible shape transformations are achieved from a single hydrogel sheet by repeatably writing in the sheet with different nanoparticle patterns. The shape transformations were verified by finite element modeling. The present strategy is simple, fast, and efficient in reprogramming the shape change of the thermoresponsive hydrogel material. The composite hydrogel sheet may find applications in soft robotics, tissue engineering, and controlled release.

**KEYWORDS:** programmable, hydrogel, shape transformation, nanoparticle pattern, composite material



## 1. INTRODUCTION

Shape-changing polymer materials (e.g., shape-memory polymer, liquid crystal elastomer, and hydrogels) have gained great attention in the past decades, owing to their diverse applications in soft robotics, biomedicine, deployable devices, actuators, and so on.<sup>1–16</sup> Most shape-changing materials are programmed to transform from a flat sheet to one or several specific three-dimensional shapes in the presence of a stimulus such as temperature,<sup>17–25</sup> pH,<sup>25–29</sup> ions,<sup>30,31</sup> DNA,<sup>32,33</sup> enzymes,<sup>34</sup> solvents,<sup>35,36</sup> humidity,<sup>37–40</sup> light,<sup>41–50</sup> and magnetic and electric fields.<sup>51–54</sup> For instance, with the incorporation of multiple distinct responsive polymer components in the hydrogel matrix, the same patterned hydrogel sheet can transform to several distinct shapes in the presence of different stimuli.<sup>55</sup> Among shape-morphing materials, the hydrogel is of particular interest due to its biocompatibility, large and reversible volume change, broad material and stimuli choices, and so on.<sup>15,56,57</sup> The shape-changing hydrogel shows promising applications in a variety of fields such as drug delivery, soft robotics, and tissue engineering.<sup>8</sup>

Dynamically reconfiguring shape changes from the same material is of paramount importance in achieving adaptive functions and sustainability.<sup>58</sup> Several strategies have been developed to achieve this goal, including (i) introducing a

reversible pattern of shape-memory phases with distinct switching temperatures in a shape-memory film;<sup>59</sup> (ii) reversibly changing the molecular state of photoabsorbing dyes integrated in the liquid crystal polymer sheet;<sup>60</sup> (iii) controlling the laser irradiation pattern on a photoresponsive hydrogel film;<sup>61,62</sup> (iv) reversibly altering the alignment of mesogens in a liquid crystal vitrimer film,<sup>63</sup> and (v) reversibly introducing metal ions in ionic hydrogels.<sup>31</sup> These strategies, however, are either limited by the number of shapes that can be transformed from a single polymer film or require a labor-intensive chemical modification of the polymer matrix. Nevertheless, there is a need of simple approaches toward reprogrammable shape transformations of hydrogel materials.

Herein we reported a new strategy to reprogram the shape transformation of hydrogel materials based on in situ generation of an erasable and rewritable pattern of iron oxide nanoparticles (IONPs) within a thermoresponsive poly(*N*-isopropylacrylamide) (PNIPAm) hydrogel matrix. The hydrogel domain loaded with IONPs shrunk upon the laser irradiation of a near-infrared light via a combination of the photothermal effect of IONPs and the thermoresponsive-

**Received:** September 14, 2019

**Accepted:** October 21, 2019

**Published:** October 21, 2019

ness of the PNIPAm hydrogel.<sup>64</sup> The patterned differential shrinkage in the composite hydrogel sheet resulted in a specific out-of-plane shape deformation of the sheet to form a desired shape. The pattern of IONPs can be erased by acid treatment, and a new pattern can be readily introduced in the same piece of hydrogel, giving rise to a distinct shape. The shape transformations were verified by finite element modeling of the patterned hydrogel sheets. The repeatable erasing and writing of IONPs enables the reprogrammable shape transformation of the material in a facile and robust manner. This strategy is simple and efficient and can be applied for other types of thermoresponsive hydrogel materials.

## 2. EXPERIMENTAL SECTION

**2.1. Materials.** All chemicals were purchased from Sigma-Aldrich unless otherwise noted, and the chemicals were used without further treatment. The chemicals used are as follows: *N*-isopropylacrylamide (NIPAm, monomer), *N,N'*-methylenebis(acrylamide) (BIS, cross-linker), ammonium persulfate (APS, initiator), *N,N,N',N'*-tetramethylethylenediamine (TEMED, catalyst), iron (III) chloride, iron (II) chloride, sodium hydroxide (NaOH), hydrochloric acid (HCl, 36–38%). The adhesive Loctite 406 was bought from Henkel. The agarose powder was purchased from EZ BioResearch. The polydimethylsiloxane (PDMS) elastomer kit (Sylgard 184) was bought from Dow Corning. Deionized water was used throughout the experiments.

**2.2. Synthesis of PNIPAm Hydrogel.** The PNIPAm hydrogel was fabricated by a redox method. Typically, 0.113 g of NIPAm monomer and 0.006 g of BIS cross-linker were dissolved in 1 mL of water. After 10  $\mu$ L of 10 wt % APS aqueous solution was added, the hydrogel precursor solution was purged with nitrogen for 5 min. Then, 5  $\mu$ L of TEMED was added and mixed with the monomer solution. After mixing, the monomer solution was injected into a premade mold made of two cover slides and spacers. The gelation was allowed to proceed at room temperature for 2 h. Then, the hydrogel sheet was removed from the mold and was immersed in a large amount of water to leak out unreacted materials. To fabricate the PNIPAm hydrogel tube, the hydrogel precursor was injected to a self-made tubular mold.

**2.3. Fabrication of Agarose Stamp.** The agarose stamp was made by gelating agarose aqueous solution on a PDMS mold. In a representative fabrication process, a poly(lactic acid) (PLA) plastic mold with bas-relief features was first printed out by using a 3D printer (Original Prusa i3MK2S). Then, the PDMS was cured on this mold at 70 °C for 1 h. The cured PDMS with opposite features was peeled off from the PLA mold. After that, the surface of the PDMS mold was made hydrophilic by subjecting it to an air plasma for 3 min. Then, 4 wt % hot agarose aqueous solution was casted onto the PDMS mold and was cooled at room temperature to gelate. After gelation, the agarose gel with bas-relief features was peeled off from the PDMS mold. This agarose gel was then used in the wet-stamping process.

**2.4. Wet Stamping.** An aqueous layer of iron ion solution was formed on the surface of agarose gel by drop-casting the ion solution onto the agarose gel. The aqueous layer was kept on the agarose gel for 2 min for ions to diffuse into the agarose gel. Then, the aqueous ion layer was wiped off from the agarose gel using a Kimwipe. The agarose stamp was then brought in contact with the surface of the PNIPAm hydrogel for 1 min to deliver iron ions to the PNIPAm hydrogel. Thereafter, a 0.5 M NaOH solution was sprayed onto the PNIPAm hydrogel using a spray bottle. The NaOH solution was kept on the PNIPAm hydrogel for 1 min to coprecipitate the Fe<sup>3+</sup> and Fe<sup>2+</sup> to generate IONPs. Finally, the IONP-loaded PNIPAm hydrogel (i.e., composite hydrogel) was kept in water for the shape transformation study. By designing features in the agarose stamp, different IONP patterns in the hydrogel could be easily obtained. To erase IONPs, a concentrated HCl solution was sprayed onto the hydrogel, which dissolved the IONPs within 1 min. After spraying water onto the

hydrogel to remove excess HCl and iron ions, new nanoparticle patterns can be written in the same sheet.

To study the IONP domain size as a function of the iron ion diffusion time, the ion-inked agarose stamp was brought in contact with the PNIPAm hydrogel for different amounts of time. Then, the ion-loaded PNIPAm hydrogel was immersed in a 0.5 M NaOH solution for 2 min to generate IONPs. The size of the generated nanoparticle domain in both the *xy*- and *z*-directions of the hydrogel was then analyzed by using an optical microscope. The IONP domain size was plotted with respect to the stamping (ion diffusion) time.

**2.5. Deformation of Hydrogel.** An 808 nm laser (MDL-N-808, Changchun New Industries Optoelectronics Technology Co., Ltd., China) with a tunable output power (0–8 W) was used as the laser source throughout the experiments. During the experiments, the composite hydrogel was immersed in 600 mL of water in a glass Petri dish. To study the bending deformation under laser irradiation, the hydrogel sheet was patterned with an IONP stripe with a varied width, which was then exposed to the laser. The length, width, and thickness of the hydrogel were 20, 4, and 0.25 mm, respectively, without special notification.

**2.6. Regulation of Chemical Release.** The composite hydrogel sheet was used as a “smart gate” to regulate the chemical (rhodamine B) release through its bending and unbending, which was controlled by the laser light. A hollow cavity with a circular shape (diameter: 6 mm) was made in a gelatin hydrogel, and then, a rhodamine B aqueous solution (0.1 mM) was added to the cavity. After that, the composite hydrogel sheet was partly glued using a cyanoacrylate-based adhesive onto the gelatin hydrogel, covering the rhodamine B-loaded region. Subsequently, the hydrogel device was immersed in 600 mL of water in a glass Petri dish, and the composite hydrogel sheet was exposed to the laser at a power density of 6.38 W/cm<sup>2</sup>.

**2.7. Measurements.** The swelling property of the hydrogel was characterized by measuring its dimensions change as a function of the temperature. A disc-shaped pure or IONP-loaded hydrogel was immersed in a water bath with a set temperature for 1 day, and its diameter was measured and then plotted with respect to the temperature.

An AR2000 stress-controlled rheometer (TA Instruments) was used to study the mechanical properties of the pure and composite hydrogel sheets. Rheological experiments were performed at 25 and 34 °C, individually, by using a cone-and-plate geometry (20 mm diameter and 2° cone angle). A solvent trap was used to minimize the drying of the sample during the measurements. The dynamic stress-sweep experiments were first performed on the sample to identify its linear viscoelastic (LVE) region at different temperatures, and then, the dynamic frequency sweeps were performed within the LVE region.

The optical property of the composite hydrogel was characterized by measuring its light extinction using UV–vis spectroscopy (Lambda 40 UV/vis Spectrometer, PerkinElmer, USA). In the measurement, air was used as the reference, and a piece of hydrogel was then put on a glass slide. The UV–vis spectra were then taken at a slit width of 1 nm, a scanning speed of 480 nm/min, and a data interval of 1 nm.

To characterize the IONPs in the hydrogel, the composite hydrogel was first freeze-dried and then was coated with carbon (JFC-1200 Fine Coater, Japan). Following that, scanning electron microscopy (XL Series-30, Philips, USA) was used to characterize the IONPs in the hydrogel.

To measure the surface temperature of the hydrogel under the laser irradiation, a piece of pure PNIPAm hydrogel (length: 30 mm, width: 12 mm, thickness: 2 mm) was put on a plastic Petri dish (made of polystyrene) in air at the room temperature (19.5 °C). The hydrogel was irradiated by the laser with a power density (PD) of 6.38 W/cm<sup>2</sup> for 1 min. Then, the laser was switched off, and the surface temperature of the pure hydrogel was measured by using a digital thermometer. A piece of composite PNIPAm hydrogel (length: 30 mm, width: 12 mm, thickness: 2 mm) was also irradiated in air at 6.38 W/cm<sup>2</sup> for 1 min, and its surface temperature was measured in the same way as the pure hydrogel.

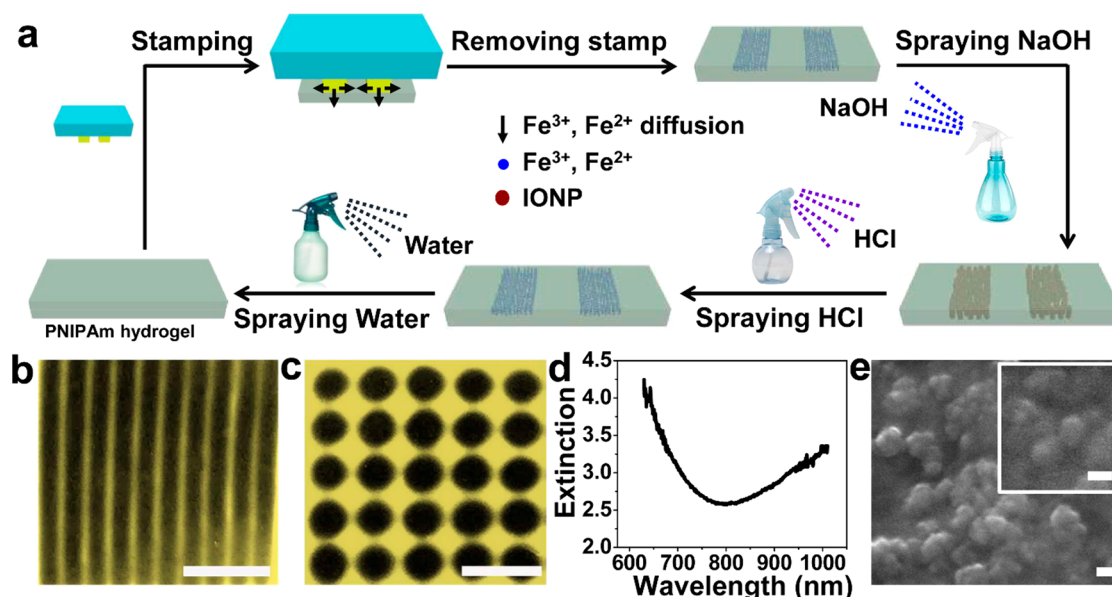


**Figure 1.** (a) Schematic illustration of the patterning, erasing, and rewriting IONPs in a thermoresponsive PNIPAm hydrogel matrix. (b,c) Representative composite hydrogel sheets with strip (b) and spot (c) patterns of IONPs. (d) UV–vis extinction spectrum of the composite hydrogel sheet. (e) SEM image of IONPs in the freeze-dried hydrogel sheet. Scale bars are 4 mm in (b,c), 100 nm in (e), and 60 nm in the inset image of (e).

### 3. RESULTS AND DISCUSSION

#### 3.1. Generation of Nanoparticle Pattern in the Hydrogel.

We developed a stamping–reacting approach to fabricate erasable and rewritable composite hydrogel sheets patterned with IONPs that served as photothermal agents. The PNIPAm hydrogel was chosen as the matrix, since it has a well-defined phase transition at its lower critical solution temperature ( $\sim 33^\circ\text{C}$ ).<sup>65</sup> During the wet-stamping process, the iron ions diffused into selective regions of the PNIPAm hydrogel. The subsequent spraying of the sodium hydroxide (NaOH) solution (0.5M) onto the PNIPAm hydrogel loaded with iron ions generated a composite hydrogel sheet regioselectively patterned with IONPs inside (Figure 1a).<sup>66–69</sup> Figure 1b,c showed two representative patterns of IONPs in the hydrogel sheets. The feature size and spacing were  $\sim 1$  mm and  $400\ \mu\text{m}$ , respectively, and the resolution of the patterning may be further improved with an optimization of the stamping protocol (Figure 1b,c). The composite hydrogel sheet exhibited a broad extinction in the UV–vis–NIR range (Figure 1d). The generated IONPs showed irregular shapes and were usually presented as aggregates in the hydrogel matrix (Figure 1e). The domain size of IONPs in both the lateral and thickness directions of the hydrogel can be modulated by controlling the stamping (ion diffusion) time and the ion concentration in the stamp (Figure 2). For example, at ion concentrations of 1 M  $\text{Fe}^{2+}$  and 2 M  $\text{Fe}^{3+}$ , the IONP domain size increased from 370 to 540  $\mu\text{m}$  in the lateral direction (Figure 2a) and from 930 to 1470  $\mu\text{m}$  in the thickness direction (z-direction) (Figure 2b), with the increase of the ion diffusion time from 1 to 2 min.

**3.2. Bending Deformation Study of Composite Hydrogel Sheet.** We evaluated the bending deformation of the composite hydrogel sheet patterned with a stripe of IONPs. We found that both IONP stripe width and laser PD needed to reach a certain threshold before a bending deformation could occur (Figure 3). With an increasing stripe width, the minimum laser PD needed for a bending to occur

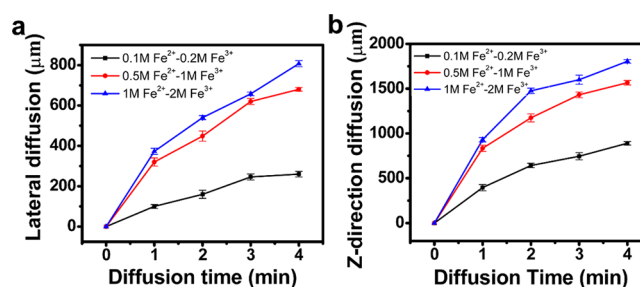


**Figure 2.** Study of the  $\text{Fe}^{3+}$ ,  $\text{Fe}^{2+}$  ion diffusion in the hydrogel during the stamping process. (a) Growth of the IONP domain size in the hydrogel's lateral ( $xy$ )-direction as a function of the ion diffusion time; (b) growth of the IONP domain size in the hydrogel's  $z$ -direction as a function of the ion diffusion time.

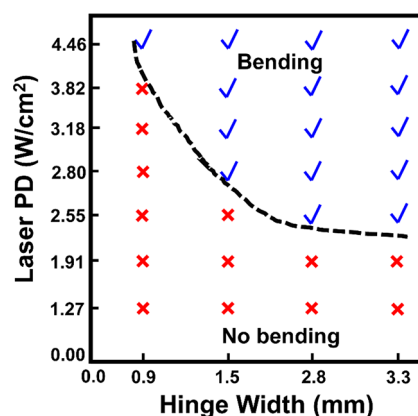


**Figure 3.** Bending analysis of the composite hydrogel sheet patterned with an IONP stripe (hinge) with respect to the hinge width and the laser PD.

was reduced. With the increase of the laser PD, the minimum stripe width required for the bending deformation decreased. When a bending deformation occurred under the NIR

irradiation (wavelength: 808 nm), the irradiated stripe area drastically shrunk due to the localized photothermal-heating-induced contraction of the hydrogel (Figures S1 and S2) and thus acted as a hinge, along which the sheet bent (Figure S3). The composite sheet gradually reached a bending angle of  $180^\circ$  with the increase of the laser irradiation time at a laser PD of  $6.38 \text{ W/cm}^2$  (Figure 4a). In addition, the maximum bending angle of the hydrogel sheet at equilibrium increased from  $67^\circ$  to  $180^\circ$  with an increasing laser PD from  $3.52$  to  $6.38 \text{ W/cm}^2$  (Figure 4b).

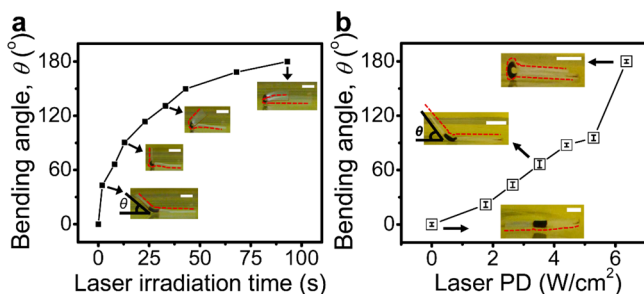


**Figure 4.** Bending angle of the composite hydrogel sheet patterned with an IONP stripe (stripe width: 3 mm) with respect to the laser irradiation time (a) and the laser PD (b). The laser PD used was  $6.38 \text{ W/cm}^2$ . The red dotted lines in the inset images were used to indicate the contour of the composite hydrogel sheet. Scale bars: 3 mm.

We systematically assessed the effect of the stripe width and the laser PD on the bending deformation of the hydrogel sheet. A bending deformation diagram was constructed, in which the parameters (hinge width and laser PD) were identified for the sheet to have a  $180^\circ$  bending angle (Figure 5). The hydrogel sheet with a larger hinge width required a smaller laser PD for the sheet to reach a bending angle of  $180^\circ$  (Figure 5).

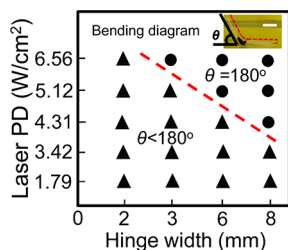


**Figure 5.** Bending diagram illustrating the condition of the IONP stripe width and the laser PD that led to bending angles of  $180^\circ$  (●) and less than  $180^\circ$  (▲) of the composite sheet. Inset is a representative optical image of the bent hydrogel sheet. The red dotted line in the inset image was used to indicate the contour of the composite hydrogel sheet. Scale bar: 3 mm.

**3.3. Reprogrammable Shape Transformation of Composite Hydrogel Sheet.** We demonstrated the reprogrammable shape transformation of the composite hydrogel sheet by varying the shapes of IONP patterns (Figure 6). The IONP patterns can be readily erased by spraying hydrochloric acid (HCl) onto the composite hydrogel sheet. After the iron and  $\text{Cl}^-$  ions were washed away with deionized water, new IONP patterns were readily stamped in the sheet. The erasing and rewriting of IONP patterns took about 5 min and ideally can be repeated for unlimited times (in our experiments, we used the hydrogel sheets for at least 20 cycles). A variety of distinct shapes were transformed from a

single sheet with varied nanoparticle patterns upon the laser irradiation (Figure 6). For example, when an IONP pattern with a triangular frame shape was used, a localized cylindrical surface was generated in the transformed sheet (Figure 6a). When using an IONP pattern of a discontinuous cross-shape, the transformed hydrogel sheet had four localized saddle-like surfaces (Figure 6b). With an IONP pattern of a square frame shape, the transformed sheet had cylindrical surfaces on its edges and had a spherical surface in the region enclosed by the IONP pattern (Figure 6c). With an IONP pattern of a concentric shape, the hydrogel sheet adopted a saddle (Figure 6d, which is in agreement with the previous work.<sup>55</sup> Many other transformations were obtained by using new nanoparticle patterns in the sheet (Figure S4). It took about 5 s to initiate the shape transformation of the patterned hydrogel sheet under the laser irradiation with a laser PD of  $6.38 \text{ W/cm}^2$  (Supplementary Video). The deformed hydrogel sheet recovered its original flat state in 15 min. In addition to patterning the planar hydrogel sheet, this patterning technique is also applicable to a nonplanar surface. As an example, an IONP region was generated in a tubular hydrogel by wrapping an ion-inked paper around the hydrogel tube, which was then subject to NaOH treatment to produce IONPs (Figure S5a). The patterned region in the tube shrunk under the laser irradiation, resulting in a necking region in the hydrogel tube (Figure S5b).

We conducted a finite element modeling simulation of the shape transformations of the composite hydrogel sheet by considering the thermodynamics of the PNIPAm hydrogel.<sup>61</sup> The deformed geometry of the composite sheet was a result of the minimization of the sheet's Helmholtz free energy composed of the free energy due to the mixing of the PNIPAm network with water and the free energy resulting from the interior stresses in the hydrogel body that had a photothermal-induced differential shrinkage in it (see Supporting Information for model details). The shape transformations of the composited sheet calculated by the finite element modeling simulation were presented in Figure 6e–h. Each IONP pattern generated a specific photothermal-induced pattern of the mechanical stress in the composite hydrogel sheet, resulting in a distinct deformation. The simulation results were in good agreement with the experimental findings.

**3.4. Regulation of Chemical Release.** We demonstrated the use of the composite hydrogel sheet as a “smart gate” in regulating the chemical release by using light (Figure 7). Rhodamine B was first loaded in the hollow cavity within a piece of gelatin hydrogel, and a circular composite hydrogel sheet patterned with a cross-shape of IONP pattern was partly glued to the gelatin hydrogel to cover the cavity (Figure 7a,b). Upon the laser irradiation, the hydrogel sheet gradually bent upward to open the “gate” (Figure 7c). With the increase of the irradiation time, rhodamine B diffused from the cavity in the gelatin hydrogel to the surrounding water through the “gate” (Figure 7d). When the laser was switched off, the bent sheet gradually recovered its original flat state to close the “gate”, blocking the diffusion of chemicals (Figure 7e,f). This “open” and “close” gating process can be repeated for many cycles to achieve time-dependent controlled release of payloads.

## 4. CONCLUSION

In conclusion, we have developed a new and robust strategy to reprogram the light-induced shape transformation of a

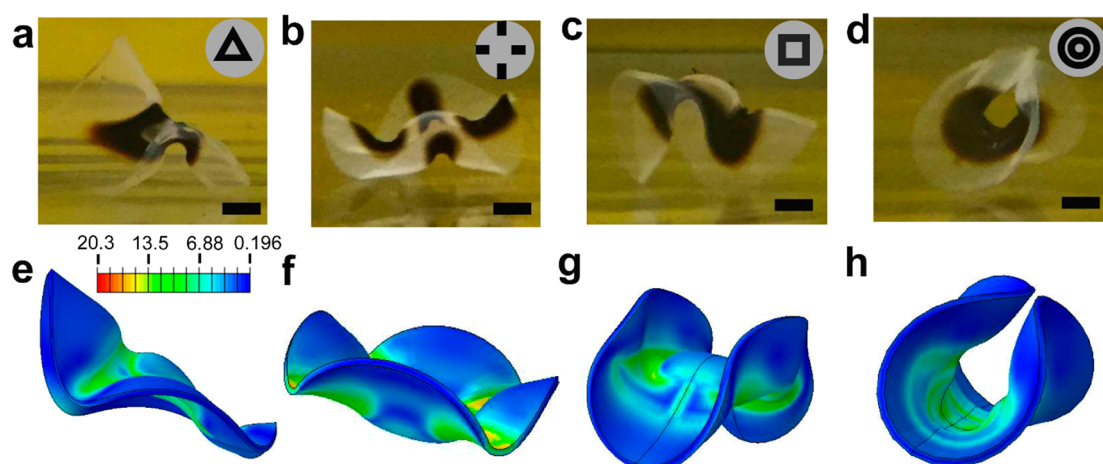


**Figure 6.** Reprogrammable shape transformation of the composite hydrogel sheet upon laser irradiation by varying the shape of the IONP patterns (black areas) in the experiments (a–d) and in the finite element modeling (FEM) simulations (e–h). Insets in (a–d) show IONP patterns (black areas) in the hydrogel. The color legend suggested the distribution of the mechanical stress calculated by FEM in the sheet under the laser irradiation. The diameter and thickness of the hydrogel disc were 13 and 0.25 mm, respectively. Scale bars are 2 mm.

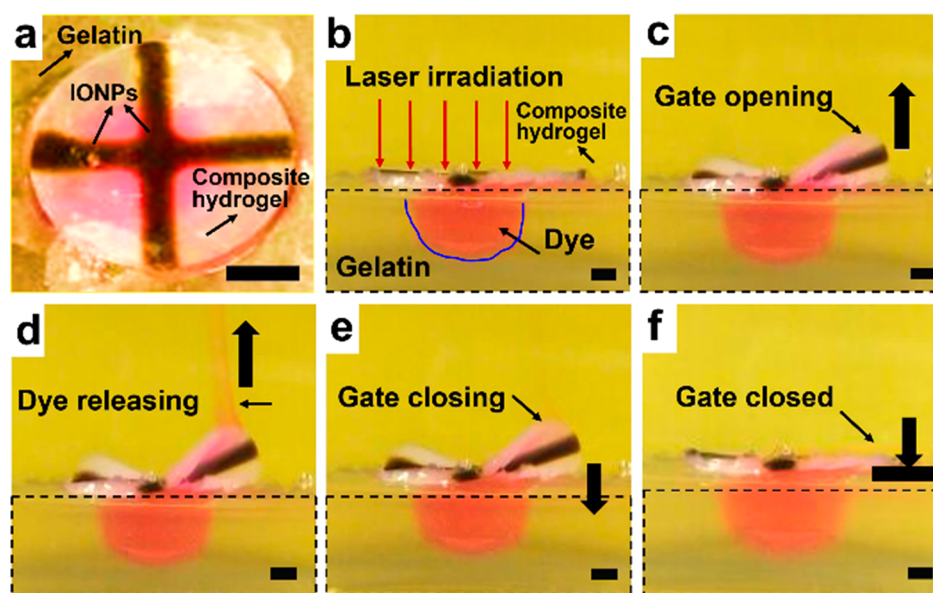


**Figure 7.** Light-regulated chemical release by using the composite hydrogel sheet as a smart gate. (a,b) Top view (a) and side view (b) of an IONP-patterned composite hydrogel sheet that covered the top of the cavity containing rhodamine B within a piece of gelatin hydrogel (enclosed by the black dashed lines). Rhodamine B was loaded in the cavity. (c–f) Controlled release of rhodamine B from the cavity in the gelatin to the surrounding water using the light-triggered deformation of the composite sheet as the gate. Scale bars are 3 mm in (a) and 1.5 mm in (b–f).

thermo-responsive composite hydrogel sheet with erasable and rewritable patterns of IONPs. Numerous distinct and reversible shape transformations were achieved from a single hydrogel sheet by writing in the sheet different nanoparticle patterns, which were verified by finite element modeling simulation. The present strategy is simple, fast, and efficient in reprogramming the shape changes of the hydrogel material, and it is expected this strategy can be extended to other thermo-responsive hydrogel systems. The composite hydrogel sheet reported in this study may find applications in soft robotics, tissue engineering, and controlled release.

## ■ ASSOCIATED CONTENT

### Supporting Information

The Supporting Information is available free of charge on the ACS Publications website at DOI: 10.1021/acsami.9b16610.

Simulation model, swelling and shear modulus property of the hydrogel, photothermal property of the hydrogel, deformation of a patterned nonplanar hydrogel, deformation of composite hydrogel sheet with other patterns of IONPs, deformation of composite hydrogel sheet with reduced sheet thickness (PDF)

(AVI)

## ■ AUTHOR INFORMATION

### Corresponding Author

\*E-mail: znie@fudan.edu.cn.

### ORCID

Srinivasa R. Raghavan: 0000-0003-0710-9845

Zhihong Nie: 0000-0001-9639-905X

## Notes

The authors declare no competing financial interest.

## ACKNOWLEDGMENTS

Z.N. gratefully acknowledges the support by the Program for Professor of Special Appointment (Eastern Scholar) at Shanghai Institutions of Higher Learning as well as the Startup Fund from Fudan University. We also acknowledge the support of the Maryland NanoCenter and its NispLab. The NispLab is supported in part by the NSF as a member of the MRSEC Shared Experimental Facilities.

## REFERENCES

- Geryak, R.; Tsukruk, V. V. Reconfigurable and actuating structures from soft materials. *Soft Matter* **2014**, *10*, 1246–1263.
- Zhao, Q.; Qi, H. J.; Xie, T. Recent progress in shape memory polymer: New behavior, enabling materials, and mechanistic understanding. *Prog. Polym. Sci.* **2015**, *49–50*, 79–120.
- Liu, Y.; Genzer, J.; Dickey, M. D. 2D or not 2D? Shape-programming polymer sheets. *Prog. Polym. Sci.* **2016**, *52*, 79–106.
- Zhang, Y. H.; Zhang, F.; Yan, Z.; Ma, Q.; Li, X. L.; Huang, Y. G.; Rogers, J. A. Printing, folding and assembly methods for forming 3D mesostructures in advanced materials. *Nat. Rev. Mater.* **2017**, *2*, 17019.
- White, T. J.; Broer, D. J. Programmable and adaptive mechanics with liquid crystal polymer networks and elastomers. *Nat. Mater.* **2015**, *14*, 1087–1098.
- Rogers, J.; Huang, Y. G.; Schmidt, O. G.; Gracias, D. H. Origami MEMS and NEMS. *MRS Bull.* **2016**, *41*, 123–129.
- van Manen, T.; Janbaz, S.; Zadpoor, A. A. Programming the shape-shifting of flat soft matter. *Mater. Today* **2018**, *21*, 144–163.
- Ionov, L. Hydrogel-based actuators: possibilities and limitations. *Mater. Today* **2014**, *17*, 494–503.
- Zhou, J.; Sheiko, S. S. Reversible shape-shifting in polymeric materials. *J. Polym. Sci., Part B: Polym. Phys.* **2016**, *54*, 1365–1380.
- Kempaiah, R.; Nie, Z. H. From nature to synthetic systems: shape transformation in soft materials. *J. Mater. Chem. B* **2014**, *2*, 2357–2368.
- Hines, L.; Petersen, K.; Lum, G. Z.; Sitti, M. Soft Actuators for Small-Scale Robotics. *Adv. Mater.* **2017**, *29*, 1603483.
- Xu, L. Z.; Shyu, T. C.; Kotov, N. A. Origami and Kirigami Nanocomposites. *ACS Nano* **2017**, *11*, 7587–7599.
- Lowenberg, C.; Balk, M.; Wischke, C.; Behl, M.; Lendlein, A. Shape-Memory Hydrogels: Evolution of Structural Principles To Enable Shape Switching of Hydrophilic Polymer Networks. *Acc. Chem. Res.* **2017**, *50*, 723–732.
- Ko, H.; Javey, A. Smart Actuators and Adhesives for Reconfigurable Matter. *Acc. Chem. Res.* **2017**, *50*, 691–702.
- Jeon, S. J.; Hauser, A. W.; Hayward, R. C. Shape-Morphing Materials from Stimuli-Responsive Hydrogel Hybrids. *Acc. Chem. Res.* **2017**, *50*, 161–169.
- Ube, T.; Ikeda, T. Photomobile Polymer Materials with Crosslinked Liquid-Crystalline Structures: Molecular Design, Fabrication, and Functions. *Angew. Chem., Int. Ed.* **2014**, *53*, 10290–10299.
- Wei, Z. J.; Jia, Z.; Athas, J. M.; Wang, C. Y.; Raghavan, S. R.; Li, T.; Nie, Z. H. Hybrid hydrogel sheets that undergo pre-programmed shape transformations. *Soft Matter* **2014**, *10*, 8157–8162.
- Morales, D.; Bharti, B.; Dickey, M. D.; Velev, O. D. Bending of Responsive Hydrogel Sheets Guided by Field-Assembled Micro-particle Endoskeleton Structures. *Small* **2016**, *12*, 2283–2290.
- Kularatne, R. S.; Kim, H.; Ammanamanchi, M.; Hayenga, H. N.; Ware, T. H. Shape-Morphing Chromonic Liquid Crystal Hydrogels. *Chem. Mater.* **2016**, *28*, 8489–8492.
- Stoychev, G.; Reuther, C.; Diez, S.; Ionov, L. Controlled Retention and Release of Biomolecular Transport Systems Using Shape-Changing Polymer Bilayers. *Angew. Chem., Int. Ed.* **2016**, *55*, 16106–16109.
- Jiang, S. H.; Liu, F. Y.; Lerch, A.; Ionov, L.; Agarwal, S. Unusual and Superfast Temperature-Triggered Actuators. *Adv. Mater.* **2015**, *27*, 4865–4870.
- Zhao, Q.; Zou, W. K.; Luo, Y. W.; Xie, T. Shape memory polymer network with thermally distinct elasticity and plasticity. *Sci. Adv.* **2016**, *2*, No. e1501297.
- Xu, W. A.; Qin, Z.; Chen, C. T.; Kwag, H. R.; Ma, Q. L.; Sarkar, A.; Buehler, M. J.; Gracias, D. H. Ultrathin thermoresponsive self-folding 3D graphene. *Sci. Adv.* **2017**, *3*, No. e1701084.
- Breger, J. C.; Yoon, C.; Xiao, R.; Kwag, H. R.; Wang, M. O.; Fisher, J. P.; Nguyen, T. D.; Gracias, D. H. Self-Folding Thermo-Magnetically Responsive Soft Microgrippers. *ACS Appl. Mater. Interfaces* **2015**, *7*, 3398–3405.
- Ware, T. H.; McConney, M. E.; Wie, J. J.; Tondiglia, V. P.; White, T. J. Voxellated liquid crystal elastomers. *Science* **2015**, *347*, 982–984.
- Wu, Z. L.; Moshe, M.; Greener, J.; Therien-Aubin, H.; Nie, Z. H.; Sharon, E.; Kumacheva, E. Three-dimensional shape transformations of hydrogel sheets induced by small-scale modulation of internal stresses. *Nat. Commun.* **2013**, *4*, 1586.
- Zhao, Q.; Yang, X. X.; Ma, C. X.; Chen, D.; Bai, H.; Li, T. F.; Yang, W.; Xie, T. A bioinspired reversible snapping hydrogel assembly. *Mater. Horiz.* **2016**, *3*, 422–428.
- Ma, C.; Li, T.; Zhao, Q.; Yang, X.; Wu, J.; Luo, Y.; Xie, T. Supramolecular Lego assembly towards three-dimensional multi-responsive hydrogels. *Adv. Mater.* **2014**, *26*, S665–S669.
- Ma, C. X.; Le, X. X.; Tang, X. L.; He, J.; Xiao, P.; Zheng, J.; Xiao, H.; Lu, W.; Zhang, J. W.; Huang, Y. J.; Chen, T. A Multiresponsive Anisotropic Hydrogel with Macroscopic 3D Complex Deformations. *Adv. Funct. Mater.* **2016**, *26*, 8670–8676.
- Athas, J. C.; Nguyen, C. P.; Kummar, S.; Raghavan, S. R. Cation-induced folding of alginate-bearing bilayer gels: an unusual example of spontaneous folding along the long axis. *Soft Matter* **2018**, *14*, 2735–2743.
- Palleau, E.; Morales, D.; Dickey, M. D.; Velev, O. D. Reversible patterning and actuation of hydrogels by electrically assisted ionoprinting. *Nat. Commun.* **2013**, *4*, 2257.
- Cangialosi, A.; Yoon, C.; Liu, J.; Huang, Q.; Guo, J. K.; Nguyen, T. D.; Gracias, D. H.; Schulman, R. DNA sequence-directed shape change of photopatterned hydrogels via high-degree swelling. *Science* **2017**, *357*, 1126–1129.
- Shim, T. S.; Estephan, Z. G.; Qian, Z. X.; Prosser, J. H.; Lee, S. Y.; Chenoweth, D. M.; Lee, D.; Park, S. J.; Crocker, J. C. Shape changing thin films powered by DNA hybridization. *Nat. Nanotechnol.* **2017**, *12*, 41–47.
- Athas, J. C.; Nguyen, C. P.; Zarket, B. C.; Gargava, A.; Nie, Z. H.; Raghavan, S. R. Enzyme-Triggered Folding of Hydrogels: Toward a Mimic of the Venus Flytrap. *ACS Appl. Mater. Interfaces* **2016**, *8*, 19066–19074.
- Zhao, Q.; Dunlop, J. W. C.; Qiu, X. L.; Huang, F. H.; Zhang, Z. B.; Heyda, J.; Dzubiella, J.; Antonietti, M.; Yuan, J. Y. An instant multi-responsive porous polymer actuator driven by solvent molecule sorption. *Nat. Commun.* **2014**, *5*, 4293.
- Deng, H.; Dong, Y.; Su, J. W.; Zhang, C.; Xie, Y. C.; Zhang, C.; Maschmann, M. R.; Lin, Y. Y.; Lin, J. Bioinspired Programmable Polymer Gel Controlled by Swellable Guest Medium. *ACS Appl. Mater. Interfaces* **2017**, *9*, 30900–30908.
- Arazoe, H.; Miyajima, D.; Akaike, K.; Araoka, F.; Sato, E.; Hikima, T.; Kawamoto, M.; Aida, T. An autonomous actuator driven by fluctuations in ambient humidity. *Nat. Mater.* **2016**, *15*, 1084–1089.
- Zhang, L. D.; Liang, H. R.; Jacob, J.; Naumov, P. Photogated humidity-driven motility. *Nat. Commun.* **2015**, *6*, 7429.
- de Haan, L. T.; Verjans, J. M. N.; Broer, D. J.; Bastiaansen, C. W. M.; Schenning, A. Humidity-Responsive Liquid Crystalline Polymer Actuators with an Asymmetry in the Molecular Trigger That Bend, Fold, and Curl. *J. Am. Chem. Soc.* **2014**, *136*, 10585–10588.

- (40) Zhang, L. D.; Chizhik, S.; Wen, Y. Z.; Naumov, P. Directed Motility of Hygroresponsive Biomimetic Actuators. *Adv. Funct. Mater.* **2016**, *26*, 1040–1053.
- (41) Mu, J. K.; Hou, C. Y.; Wang, H. Z.; Li, Y. G.; Zhang, Q. H.; Zhu, M. F. Origami-inspired active graphene-based paper for programmable instant self-folding walking devices. *Sci. Adv.* **2015**, *1*, No. e1500533.
- (42) Liu, Y.; Shaw, B.; Dickey, M. D.; Genzer, J. Sequential self-folding of polymer sheets. *Sci. Adv.* **2017**, *3*, No. e1602417.
- (43) Lv, J. A.; Liu, Y. Y.; Wei, J.; Chen, E. Q.; Qin, L.; Yu, Y. L. Photocontrol of fluid slugs in liquid crystal polymer microactuators. *Nature* **2016**, *537*, 179–184.
- (44) Gelebart, A. H.; Jan Mulder, D.; Varga, M.; Konya, A.; Vantomme, G.; Meijer, E. W.; Selinger, R. L. B.; Broer, D. J. Making waves in a photoactive polymer film. *Nature* **2017**, *546*, 632–636.
- (45) Wie, J. J.; Shankar, M. R.; White, T. J. Photomotility of polymers. *Nat. Commun.* **2016**, *7*, 13260.
- (46) Takashima, Y.; Hatanaka, S.; Otsubo, M.; Nakahata, M.; Kakuta, T.; Hashidzume, A.; Yamaguchi, H.; Harada, A. Expansion-contraction of photoresponsive artificial muscle regulated by host-guest interactions. *Nat. Commun.* **2012**, *3*, 1270.
- (47) Iamsaard, S.; Asshoff, S. J.; Matt, B.; Kudernac, T.; Cornelissen, J.; Fletcher, S. P.; Katsonis, N. Conversion of light into macroscopic helical motion. *Nat. Chem.* **2014**, *6*, 229–235.
- (48) Wang, E.; Desai, M. S.; Lee, S. W. Light-controlled graphene-elastin composite hydrogel actuators. *Nano Lett.* **2013**, *13*, 2826–2830.
- (49) Deng, J.; Li, J. F.; Chen, P. N.; Fang, X.; Sun, X. M.; Jiang, Y. S.; Weng, W.; Wang, B. J.; Peng, H. S. Tunable Photothermal Actuators Based on a Pre-programmed Aligned Nanostructure. *J. Am. Chem. Soc.* **2016**, *138*, 225–230.
- (50) Lu, X. L.; Guo, S. W.; Tong, X.; Xia, H. S.; Zhao, Y. Tunable Photocontrolled Motions Using Stored Strain Energy in Malleable Azobenzene Liquid Crystalline Polymer Actuators. *Adv. Mater.* **2017**, *29*, 1606467.
- (51) Morales, D.; Palleau, E.; Dickey, M. D.; Velev, O. D. Electro-actuated hydrogel walkers with dual responsive legs. *Soft Matter* **2014**, *10*, 1337–1348.
- (52) Yang, C.; Wang, W.; Yao, C.; Xie, R.; Ju, X. J.; Liu, Z.; Chu, L. Y. Hydrogel Walkers with Electro-Driven Motility for Cargo Transport. *Sci. Rep.* **2015**, *5*, 13622.
- (53) Kim, J.; Chung, S. E.; Choi, S. E.; Lee, H.; Kim, J.; Kwon, S. Programming magnetic anisotropy in polymeric microactuators. *Nat. Mater.* **2011**, *10*, 747–752.
- (54) Han, D.; Farino, C.; Yang, C.; Scott, T.; Browe, D.; Choi, W.; Freeman, J. W.; Lee, H. Soft Robotic Manipulation and Locomotion with a 3D Printed Electroactive Hydrogel. *ACS Appl. Mater. Interfaces* **2018**, *10*, 17512–17518.
- (55) Therien-Aubin, H.; Wu, Z. L.; Nie, Z. H.; Kumacheva, E. Multiple Shape Transformations of Composite Hydrogel Sheets. *J. Am. Chem. Soc.* **2013**, *135*, 4834–4839.
- (56) Zhang, Y. S.; Khademhosseini, A. Advances in engineering hydrogels. *Science* **2017**, *356*, eaaf3627.
- (57) Ionov, L. Biomimetic Hydrogel-Based Actuating Systems. *Adv. Funct. Mater.* **2013**, *23*, 4555–4570.
- (58) Kuksenok, O.; Balazs, A. C. Modeling the Photoinduced Reconfiguration and Directed Motion of Polymer Gels. *Adv. Funct. Mater.* **2013**, *23*, 4601–4610.
- (59) Kohlmeyer, R. R.; Buskohl, P. R.; Deneault, J. R.; Durstock, M. F.; Vaia, R. A.; Chen, J. Shape-Reprogrammable Polymers: Encoding, Erasing, and Re-Encoding. *Adv. Mater.* **2014**, *26*, 8114–8119.
- (60) Gelebart, A. H.; Mulder, D. J.; Vantomme, G.; Schenning, A.; Broer, D. J. A Rewritable, Reprogrammable, Dual Light-Responsive Polymer Actuator. *Angew. Chem., Int. Ed.* **2017**, *56*, 13436–13439.
- (61) Guo, H. Y.; Cheng, J.; Wang, J. Y.; Huang, P.; Liu, Y. J.; Jia, Z.; Chen, X. Y.; Sui, K. Y.; Li, T.; Nie, Z. H. Reprogrammable ultra-fast shape-transformation of macroporous composite hydrogel sheets. *J. Mater. Chem. B* **2017**, *5*, 2883–2887.
- (62) Hauser, A. W.; Evans, A. A.; Na, J. H.; Hayward, R. C. Photothermally Reprogrammable Buckling of Nanocomposite Gel Sheets. *Angew. Chem., Int. Ed.* **2015**, *54*, 5434–5437.
- (63) Yang, Y.; Pei, Z. Q.; Li, Z.; Wei, Y.; Ji, Y. Making and Remaking Dynamic 3D Structures by Shining Light on Flat Liquid Crystalline Vitrimers without a Mold. *J. Am. Chem. Soc.* **2016**, *138*, 2118–2121.
- (64) Huang, H. W.; Sakar, M. S.; Petruska, A. J.; Pane, S.; Nelson, B. J. Soft micromachines with programmable motility and morphology. *Nat. Commun.* **2016**, *7*, 12263.
- (65) Yu, C. J.; Duan, Z.; Yuan, P. X.; Li, Y. H.; Su, Y. W.; Zhang, X.; Pan, Y. P.; Dai, L. L.; Nuzzo, R. G.; Huang, Y. G.; Jiang, H. Q.; Rogers, J. A. Electronically Programmable, Reversible Shape Change in Two- and Three-Dimensional Hydrogel Structures. *Adv. Mater.* **2013**, *25*, 1541–1546.
- (66) Ahn, T.; Kim, J. H.; Yang, H. M.; Lee, J. W.; Kim, J. D. Formation Pathways of Magnetite Nanoparticles by Coprecipitation Method. *J. Phys. Chem. C* **2012**, *116*, 6069–6076.
- (67) Laurent, S.; Forge, D.; Port, M.; Roch, A.; Robic, C.; Vander Elst, L.; Muller, R. N. Magnetic iron oxide nanoparticles: Synthesis, stabilization, vectorization, physicochemical characterizations, and biological applications. *Chem. Rev.* **2008**, *108*, 2064–2110.
- (68) Bannerman, A. D.; Li, X. Y.; Wan, W. K. A 'degradable' poly(vinyl alcohol) iron oxide nanoparticle hydrogel. *Acta Biomater.* **2017**, *58*, 376–385.
- (69) Hernandez, R.; Criado, M.; Nogales, A.; Sprung, M.; Mijangos, C.; Ezquerro, T. A. Deswelling of Poly(N-isopropylacrylamide) Derived Hydrogels and Their Nanocomposites with Iron Oxide Nanoparticles As Revealed by X-ray Photon Correlation Spectroscopy. *Macromolecules* **2015**, *48*, 393–399.

# Supporting Information

## Programming the Shape Transformation of Composite Hydrogel Sheet via Erasable and Rewritable Nanoparticle Patterns

Hongyu Guo,<sup>†</sup> Jian Cheng,<sup>‡</sup> Kuikun Yang,<sup>†</sup> Kerry Demella,<sup>§</sup> Teng Li,<sup>‡</sup> Srinivasa R. Raghavan,<sup>§</sup> and Zhihong Nie<sup>†,\*,</sup>

<sup>†</sup>Department of Chemistry and Biochemistry, University of Maryland, College Park, MD, 20742, USA.

<sup>‡</sup>Department of Mechanical Engineering, University of Maryland, College Park, MD, 20742, USA.

<sup>§</sup>Department of Chemical and Biomolecular Engineering, University of Maryland, College Park, MD, 20742, USA.

<sup>†</sup>State Key Laboratory of Molecular Engineering of Polymers, Department of Macromolecular Science, Fudan University, Shanghai, 200438, P.R. China.

\*Corresponding author: znie@fudan.edu.cn

### Finite Element Modeling Simulation on Shape Transformations of Composite Hydrogel Sheet.

**Free energy model of temperature-responsive hydrogel.** In our PNIPAm hydrogel, the interacting aggregation of cross-linked polymer chain network and solvent molecules constitutes a thermodynamic system of which the macroscopic behaviors are governed by its thermodynamic energetics. The deformation of PNIPAm hydrogel in balance with mechanical loads and a solvent reservoir can be modeled by the framework developed by Cai and Suo.<sup>1</sup> By thermodynamics consideration, the Helmholtz free energy of a swelling hydrogel arises from two origins: (i) the stretching of the polymer network and (ii) the mixing of the two species of molecules. Hence the free energy density function takes the form:

$$W = \frac{1}{2}NkT[\mathbf{F}:\mathbf{F} - 3 - 2\log(J)] + kT\left[c\log\left(\frac{vc}{1+vc}\right) + \frac{(A_0 + B_0T)c}{1+vc} + \frac{(A_1 + B_1T)c}{(1+vc)^2}\right] \quad (1)$$

where  $W$  is the free energy per unit volume in the dry state,  $N$  is the number of polymer chains per unit volume in the dry state,  $k$  is Boltzmann constant,  $T$  is the current temperature at the material point,  $\mathbf{F}$  is the deformation gradient tensor which takes the original dry state as reference frame,  $J$  is the Jacobian of deformation gradient tensor, i.e.,  $J = \det(\mathbf{F})$ ,  $v$  is the molecular volume of water,  $c$  is the relative concentration of solvent molecules in the hydrogel-solvent aggregation, and  $A_0$ ,  $B_0$ ,  $A_1$  and  $B_1$  are parameters related to the enthalpy of mixing. The first term in Equation (1) denotes that the stretching of polymer chain network obeys a neo-Hookean hyperelastic material law, and the second term implies that the mixing of PNIPAM polymer and water molecules follows the Flory-Huggins theory of solution.  $A_0$ ,  $B_0$ ,  $A_1$  and  $B_1$  in Equation (1) are to be fitted to the experimental data for different temperature-responsive hydrogels, as we will identify in the immediate section for our composite hydrogel.

Equation (1) specifies the explicit expression of the free energy density function which takes the extensive variables  $\mathbf{F}$ ,  $c$  as well as the intensive variable  $T$  as its arguments. In such cases that

the hydrogel is put in contact with a stable aqueous reservoir, the chemical potential of solvent molecule  $\mu$  is constant; then upon Legendre transformation, the free energy density  $W$  is carried to its corresponding thermodynamic potential:

$$\hat{W}(\mathbf{F}, \mu, T|N, A_0, B_0, A_1, B_1) = W(\mathbf{F}, c, T|N, A_0, B_0, A_1, B_1) - \mu c \quad (2)$$

thus  $\hat{W}$  is a natural function of  $\mathbf{F}$ ,  $\mu$  and  $T$ .

When the stress level is adequately low so that no new void or pore is generated in the hydrogel, the volumetric change of the material solely results from the migration of solvent molecules; hence the deformation  $\mathbf{F}$  and solvent concentration  $c$  are correlated by:<sup>2</sup>

$$J = 1 + vc \quad (3)$$

Substitute Equations (1) and (3) into Equation (2), one arrives at the explicit form of  $\hat{W}$ :

$$\begin{aligned} \hat{W}(\mathbf{F}, \mu, T|N, A_0, B_0, A_1, B_1) &= \frac{1}{2}NkT[\mathbf{F}:\mathbf{F} - 3 - 2\log(J)] + \frac{kT}{v}(J - 1) \left[ \log\left(\frac{J-1}{J}\right) + \frac{(A_0 + B_0T)}{J} + \frac{(A_1 + B_1T)}{J} \right] \\ &\quad - \frac{\mu}{v}(J - 1) \end{aligned} \quad (4)$$

**Free swelling of PNIPAM hydrogel in water and determination of parameters.** When submerged in an aqueous environment with homogeneous temperature field, a piece of free standing PNIPAm hydrogel, in the absence of pre-introduced stress, will swell (or contract) freely in response to the uniformly varying temperature field. The free swelling case satisfies the condition that the hydrogel deforms uniformly in any three orthogonal directions and that the hydrogel retains its stress-free state since neither deformation mismatch nor mechanical constraint exists. For such a homogeneous deformation the principal stretch ratios have identical value, and the deformation gradient tensor becomes

$$\mathbf{F} = \begin{bmatrix} \lambda & 0 & 0 \\ 0 & \lambda & 0 \\ 0 & 0 & \lambda \end{bmatrix} \quad (5)$$

where  $\lambda$  is the uniform stretch ratio. And in this case the volumetric ratio  $J=V/V_0=\lambda^3$ , where  $V$  is the volume of the hydrogel piece in the deformed state and  $V_0$  is the volume in the reference (dry) state.

As discussed above the stress tensor vanishes:

$$S_{ik}(\mathbf{F}, \mu, T|N, A_0, B_0, A_1, B_1) = \frac{\partial \hat{W}}{\partial F_{ik}} = 0 \quad (6)$$

Equation (6) yields the relation between stretch ratio  $\lambda$  and temperature  $T$  in the free swelling case. In addition, if the chemical potential of water is known and set to zero, then  $T$  can be readily expressed by the following equation:

$$T = - \frac{N\nu(\lambda^5 - \lambda^3) + \lambda^6 \log(1 - \lambda^{-3}) + \lambda^3 + (A_0 + A_1 \lambda^{-3})}{B_0 + \lambda^{-3} B_1} \quad (7)$$

The equation above dictates the temperature required by the principle of minimum free energy, in free swelling cases, for the temperature-sensitive hydrogel to maintain certain amount of deformation. In other words it also depicts how the hydrogel deforms in response to the change of the homogeneous temperature field.

By fitting the function  $T(\lambda|S=0, \mu=0)$  to the experimentally obtained  $T \sim J$  relation, we determined the parameters  $N\nu$ ,  $A_0$ ,  $B_0$ ,  $A_1$  and  $B_1$  as  $N\nu=0.03317$ ,  $A_0=-2.5418$ ,  $B_0=0.01081$ ,  $A_1=0.57099$ ,  $B_1=-0.000418$ . We will use this set of parameters for our PNIPAM hydrogel in the following calculations.

**Model of heat transfer processes.** When the top surface is exposed to NIR laser, the IONPs embedded in PNIPAm absorb the photons and convert the light energy into heat, the surrounding hydrogel matrix is thus heated. We determined previously the thermal diffusivity of PNIPAM hydrogel  $\alpha=K/\rho C_p=2.36 \times 10^{-5}$  cm<sup>2</sup>/s, where  $K$ ,  $\rho$  and  $C_p$  denote the thermal conductivity, density, and specific heat of the material respectively.<sup>3</sup> This thermal diffusivity was used in our present study.

**Deformation of PNIPAm hydrogel in inhomogeneous temperature field.** The deformation behavior of a temperature-sensitive hydrogel is governed by a thermodynamic free energy thus resembling a hyperelastic material. Each thermodynamic equilibrium state of temperature-sensitive hydrogel is a local minimum of the system free energy which can be fully defined by the stretch ratios  $\lambda$  and a dependent solvent molecule concentration  $c$  as discussed above. Furthermore, the thermodynamic equilibrium is to be altered upon the change of environment variables. Therefore besides of being able to respond to the conventional mechanical loads, such materials as PNIPAm hydrogels are also able to deform in accordance with the change in temperature and chemical potential.

Solving for the equilibrium states is a boundary value problem (BVP). For simpler cases, e.g., free swelling hydrogel with homogeneous temperature, analytical solution can be obtained, whereas for more complicated case, e.g., hydrogel swelling in an inhomogeneous temperature field, the BVP can be solved numerically by FEM. We adopted the FEM framework established by Ding *et al.* for the temperature-responsive hydrogel,<sup>4</sup> and prescribed the material properties determined above to the PNIPAm hydrogel used in this study. At this stage we assume that the deformation of PNIPAm hydrogel will not affect the heat transfer processes. A fully coupled thermo-mechanical algorithm is implemented in the commercial FEM package ABAQUS by making use of its temperature-displacement elements.

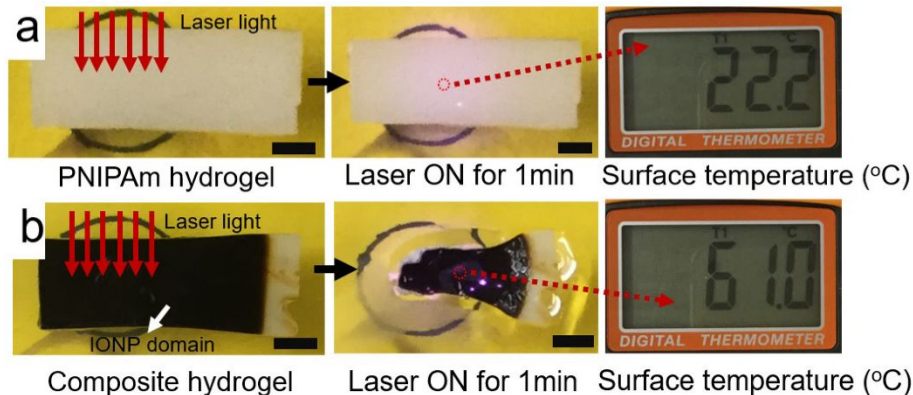


**Figure S1.** Surface temperature of pure and composite PNIPAm hydrogel under laser irradiation at  $6.38\text{W}/\text{cm}^2$  for 1minute. (a) For pure PNIPAm hydrogel, its surface temperature slightly increased under laser irradiation; (b) For composite PNIPAm hydrogel, its surface temperature increased substantially at same laser irradiation condition. Room temperature was  $19.5\text{ }^\circ\text{C}$ . Scale bar: 5mm.

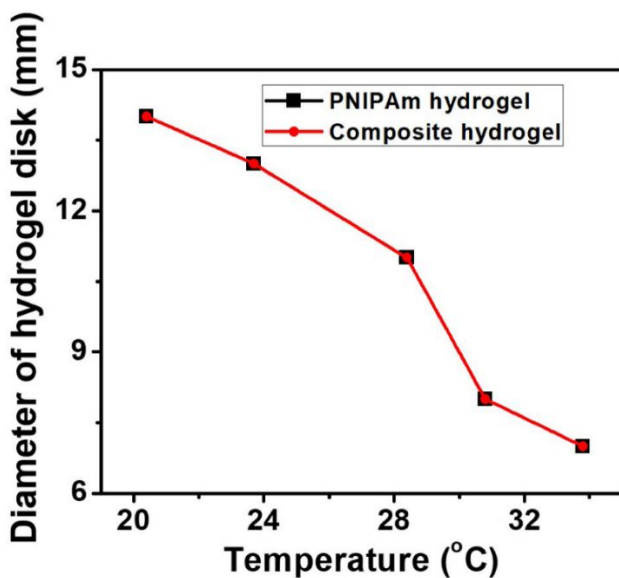


**Figure S2.** Swelling of a disc-shape hydrogel as a function of temperature. The diameter of the hydrogel disc was measured and plotted against temperature.

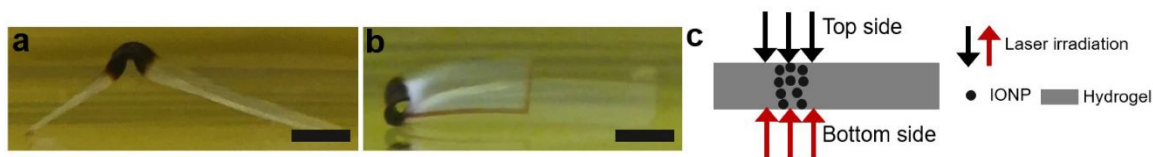


**Figure S3.** Bending of the composite hydrogel sheet under laser irradiation. (a) The hydrogel sheet bent downwards when laser was irradiated onto the bottom side of the hydrogel (red arrows in (c)); (b) the same sheet bent upwards when laser was irradiated onto the top side of the hydrogel (black arrows in (c)); This side was in contact with agarose stamp during ion diffusion. Scale bars: 3mm.

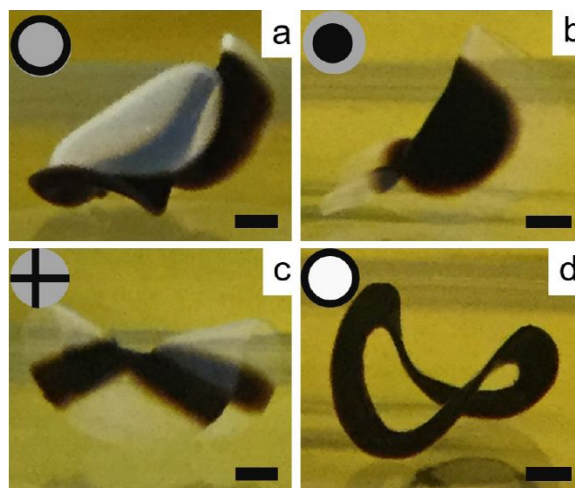


**Figure S4.** (a-c) Shape transformation of composite hydrogel sheet with varied IONP patterns. Insets in (a-c) are illustrations of sheet patterned with IONPs, in which composite hydrogel domain was colored black and pure hydrogel domain shown in grey; (d) shape deformation of a ring-shaped hydrogel with IONP pattern along hydrogel's circumference. Scale bars: 2mm.

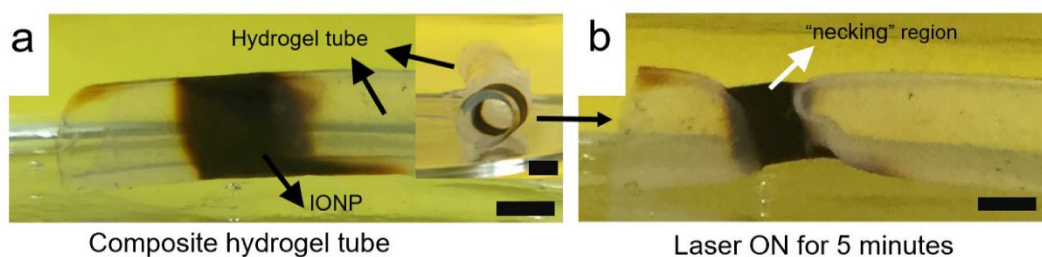


**Figure S5.** (a) PNIPAm hydrogel tube was patterned with IONPs (black areas); (b) the hydrogel tube necked in region having IONPs under laser irradiation for 5 minutes. Scale bars: 3mm.

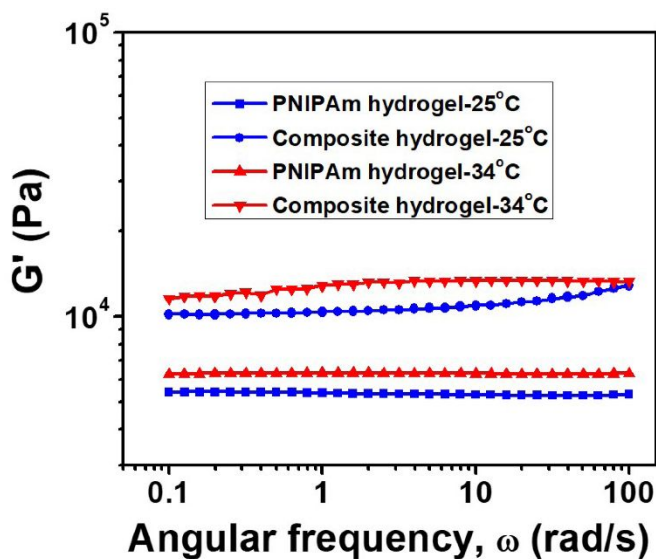


**Figure S6.** Shear modulus of pure and composite PNIPAm hydrogel as a function of temperature.

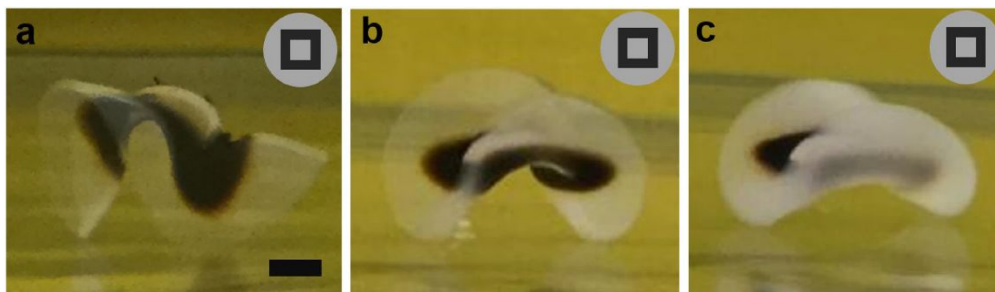


**Figure S7.** Shape transformation of composite hydrogel sheet with varied thickness. IONP domain was colored black in the hydrogel. The diameter of the hydrogel disc is 13mm. Thickness of hydrogel is: (a) 0.25mm; (b) 0.5mm; (c) 1mm. The composite hydrogel sheet was irradiated for 1min at  $6.38\text{W}/\text{cm}^2$ . Scale bar: 2mm.

- (1) Cai, S. Q.;Suo, Z. G. Mechanics and chemical thermodynamics of phase transition in temperature-sensitive hydrogels. *J. Mech. Phys. Solids* **2011**, *59*, 2259-2278.
- (2) Hong, W.; Liu, Z. S.;Suo, Z. G. Inhomogeneous swelling of a gel in equilibrium with a solvent and mechanical load. *Int. J. Solids Struct.* **2009**, *46*, 3282-3289.
- (3) Guo, H. Y.; Cheng, J.; Wang, J. Y.; Huang, P.; Liu, Y. J.; Jia, Z.; Chen, X. Y.; Sui, K. Y.; Li, T.;Nie, Z. H. Reprogrammable ultra-fast shape-transformation of macroporous composite hydrogel sheets. *J. Mater. Chem. B* **2017**, *5*, 2883-2887.
- (4) Ding, Z. W.; Liu, Z. S.; Hu, J. Y.; Swaddiwudhipong, S.;Yang, Z. Z. Inhomogeneous large deformation study of temperature-sensitive hydrogel. *Int. J. Solids Struct.* **2013**, *50*, 2610-2619.